

In Vitro and in Vivo Magnetic Resonance Detection of Tumor Cells by Targeting Glutamine Transporters with Gd-Based Probes

Simonetta Geninatti Crich,^{†,||} Claudia Cabella,[‡] Alessandro Barge,^{§,||} Simona Belfiore,^{†,||} Cristina Ghirelli,[‡] Luciano Lattuada,[#] Stefania Lanzardo,[⊥] Armando Mortillaro,^{†,||} Lorenzo Tei,^{†,||} Massimo Visigalli,[‡] Guido Forni,[⊥] and Silvio Aime^{*,†,||}

Department of Chemistry I.F.M., University of Torino, Via P. Giuria 7, Torino, 10125, Italy, Center for Molecular Imaging (CIM), University of Torino, Via P. Giuria 15, Torino, 10125, Italy, CRM Bracco Imaging S.p.A., c/o Bioindustry Park Canavese, Via Ribes 5, Collettero Giacosa, Italy, Department of Drug Science and Technology, University of Torino, Via P. Giuria 9, Torino, 10125, Italy, CRM Bracco Imaging S.p.A., Via Folli 50, Milan, Italy, and Department of Clinical and Biological Sciences, University of Torino, 10043 Orbassano, Italy

Received February 1, 2006

The glutamine transporting system is up-regulated in tumor cells because cell proliferation requires the uptake of large quantities of glutamine. It has been found that the paramagnetic magnetic resonance imaging (MRI) reporter Gd-DOTAMA-C₆-Gln, where the glutamine residue is covalently bound to the Gd chelate through a C₆ spacer, accumulates in tumor cells both “in vitro” and “in vivo” experiments. The observation that the relaxivity of cellular pellets does not increase with the increase in the amounts of entrapped Gd chelate is taken as an indication that the internalization has occurred through receptor mediated endocytosis. The iv administration of Gd-DOTAMA-C₆-Gln allowed the MRI visualization of tumor masses in A/J mice grafted with the murine neuroblastoma cell line Neuro-2a and in Her-2/neu transgenic mice developing multiple mammary carcinoma, respectively.

Introduction

The superb anatomical resolution of magnetic resonance (MR) images has made this methodology the technique of choice in modern diagnostic investigations.¹ Nowadays, more than 35% of clinical scans are performed with the administration of contrast agents (CA), which are chemicals able to amplify the contrast in the image to obtain a better discrimination between pathological regions and normal tissues. Since the endogenous contrast in a MR image arises mostly from differences in the relaxation times of tissue water protons, the contrast agents that are routinely used in clinical practice are mainly paramagnetic chelates of Gd³⁺ ions.^{2–4} Their action is based on the enhancement of the tissue contrast by increasing the longitudinal relaxation rate of water protons (1/T₁).

To date, all commercially approved gadolinium (Gd) compounds are extracellular agents with an aspecific biodistribution. The next generation of contrast agents will include systems able to recognize specific molecules on the cellular surface that act as early reporters of a given pathology. The targeting of overexpressed membrane receptors with specific radiopharmaceuticals^{5–7} is already a well-established diagnostic method in nuclear medicine for several types of tumors. However, despite its high sensitivity, this approach suffers from a poor image resolution.

In the case of MRI, this targeting strategy is hampered by the very low concentration of such receptors^{8,9} and by the relatively low sensitivity of Gd complexes with respect to the tracers used in other diagnostic techniques (i.e., SPECT, PET, optical imaging). To overcome this limitation, it is necessary

to accumulate a large number of imaging reporters at the target site by recognizing specific molecules overexpressed in the given pathology. The $\alpha_v\beta_3$ integrin receptor is an example of a neovascular target overexpressed on tumoral endothelium currently subjected to intense scrutiny in molecular imaging applications. Liposomes and nanoparticles labeled with Gd chelates and targeted to $\alpha_v\beta_3$ receptors have been used to image the neovasculature in angiogenic tumors.^{10–13} Another important target for tumor prognosis is the HER-2/neu tyrosine kinase receptor expressed on the surface of breast cancer cells. This receptor has been visualized using either targeted iron oxide nanoparticles^{14,15} or an avidin–Gd-DTPA conjugate.¹⁶ Furthermore, pegylated paramagnetic immunoliposomes carrying anti-E-selectin monoclonal antibody are used in order to identify the endothelial cells of the human umbilical vein¹⁷ (HUVEC).

In this study, we have exploited the amino acid transporting system as an alternative route to deliver a large number of Gd(III) contrast agents to the tumor cells. In fact, proliferating cells consume more glucose and amino acids (and their derivatives) than their benign counterparts.¹⁸ Transport of glucose and amino acids into cells is mediated by specific membrane proteins called transporters, which are responsible for the translocation of the substrate from one side of the membrane to the other. The increased expression or up-regulation of these transporters correlates with the greater transport of glucose and amino acids, and it is strictly related to the cells' growth. The increased glucose and amino acid uptake by tumors is often exploited by radiologists for tumor detection and staging, before and after therapeutic treatment, using radiolabeled glucose^{19,20} and amino acids^{21,22} (SPECT, PET, etc...). Furthermore, a phenylalanine derivative containing boron has been selected for neutron capture therapy applications.^{23–24} Recently, Luciani and co-workers²⁵ showed that pegylated paramagnetic liposomes bearing a glucose conjugate are taken up by tumor cells through glucose receptors (GLUT1) and visualized by MR imaging in the human carcinoma xenograft model. Our studies have been centered on the exploitation of the glutamine transport system in order to

* To whom correspondence should be addressed. Address: Department of Chemistry I.F.M., University of Torino, Via P. Giuria 7, Torino, 10125, Italy. Phone: +390116707520. Fax: +390116707855. E-mail: silvio.aime@unito.it.

[†] Department of Chemistry I.F.M., University of Torino.

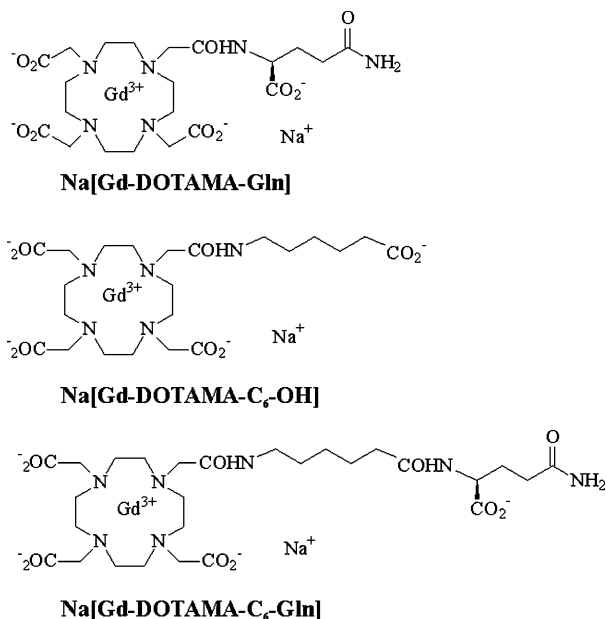
^{||} Center for Molecular Imaging (CIM), University of Torino.

[‡] CRM Bracco Imaging S.p.A., Collettero Giacosa, Italy.

[§] Department of Drug Science and Technology, University of Torino.

[#] CRM Bracco Imaging S.p.A., Milan, Italy.

[⊥] Department of Clinical and Biological Sciences, University of Torino.

Scheme 1. Schematic Representation of the Gd-DOTAMA-Gln, Gd-DOTAMA-C₆-OH, Gd-DOTAMA-C₆-Gln Complexes

incorporate many Gd units into target cells. In fact, glutamine is the most abundant amino acid in the body (0.5–0.8 mM in serum)²⁶ and is the physiological nontoxic ammonium vehicle between different mammalian tissues; therefore, glutamine is the main source of nitrogen for tumor cells that transport glutamine at a faster rate than normal cells.^{26–32} For these reasons two new DOTA derivatives (Scheme 1) functionalized with a glutamine unit have been synthesized and tested “in vitro” on different tumor cell lines and “in vivo” on cancer prone mice transgenic for rat Her-2/neu³³ and A/J mice grafted with a neuroblastoma cell line.

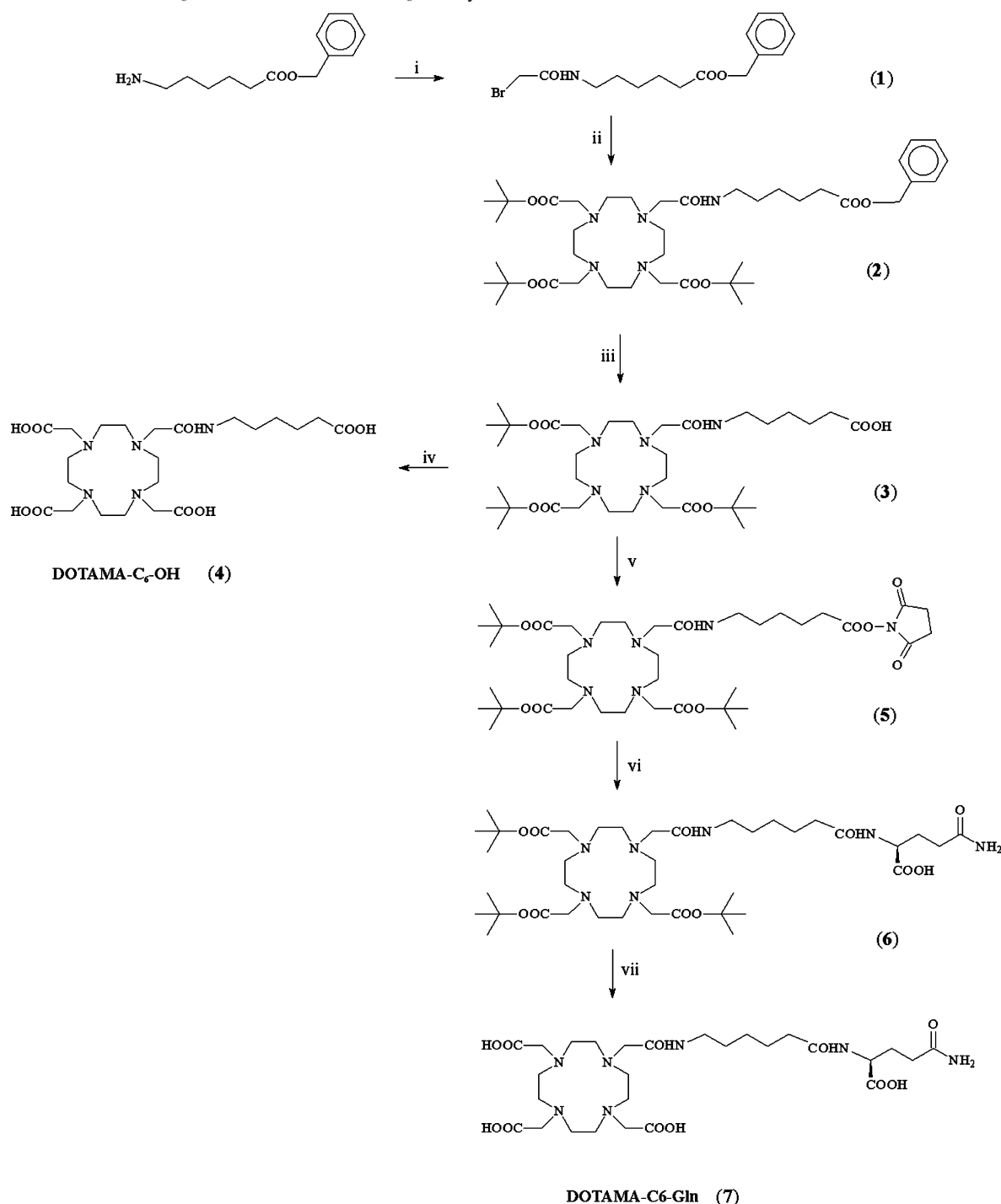
Results

Synthesis of the Ligands. While Gd-DOTAMA-Gln was synthesized accordingly to a previously reported procedure,³⁴ DOTAMA-C₆-Gln was obtained by a coupling reaction between the NHS activated ester of DOTAMA(*t*BuO)₃-C₆-OH and the unprotected L-glutamine in a homogeneous mixture of CH₃CN and a phosphate buffer at pH 8 (Scheme 2). The final ligand was obtained by the deprotection of *tert*-butyl esters in the presence of trifluoroacetic acid and CH₂Cl₂ (1:1) with an overall yield of about 50%. DOTAMA-C₆-OH was obtained by the deprotection of *tert*-butyl esters in the presence of trifluoroacetic acid and CH₂Cl₂ (1:1) of DOTAMA(*t*BuO)₃-C₆-OH with an overall yield of about 75%. Gd(III) complexes were synthesized in water by stoichiometric additions of GdCl₃ at pH 6.5. The occurrence of residual Gd³⁺ free ion was assessed by UV–vis spectroscopy using the xylenol orange method.³⁵ All complexes used in this work were shown to contain less than 0.3% (mol/mol) of residual free Gd³⁺ ion. The excess of unchelated Gd³⁺ ions was removed by the repeated alkalization of the solutions containing the metal complexes followed by centrifugation (7000 rpm).

Relaxometric Characterization of the Gd Complexes. The relaxivities (the proton relaxation enhancement of water protons in the presence of the paramagnetic complex at 1 mM) measured at 20 MHz and 298 K of Gd-DOTAMA-C₆-OH, Gd-DOTAMA-Gln, and Gd-DOTAMA-C₆-Gln were 5.0, 5.0, and 5.5 mM⁻¹ s⁻¹, respectively. These values were slightly higher than that reported for the parent Gd-DOTA complex ($r_{1p} = 4.7 \text{ mM}^{-1}$

s⁻¹)⁴ as a consequence of their increased molecular weight. The exchange rate ($k_{ex} = 1/\tau_M$) of the inner-sphere water has been determined by measuring the transverse relaxation time of ¹⁷O nuclei of solvent water molecules as a function of temperature and by fitting the obtained data to the values calculated on the basis of the Swift–Connick theory.³⁶ Gd-DOTAMA-C₆-OH, Gd-DOTAMA-Gln, and Gd-DOTAMA-C₆-Gln displayed a similar τ_m values of ~1.3 μ s at 298 K (Table 1), in agreement with those previously reported for a number of analogous Gd complexes with variously substituted DOTA-monoamide ligands.² After τ_M was independently measured, the various parameters affecting the observed proton relaxivity (r_{1p}) can be assessed by analyzing the dependence of the water ¹H relaxation rates as a function of the applied magnetic field (1/T₁ NMRD profile). The best fit values of the data calculated on the basis of the Solomon–Bloembergen–Morgan equations³⁷ (for the inner sphere contribution) and of Freed’s equation³⁸ (for the outer sphere contribution) are reported in Table 1. All complexes (Gd-DOTAMA-C₆-OH, Gd-DOTAMA-Gln, and Gd-DOTAMA-C₆-Gln) displayed a constant r_{1p} value in the pH range from 12 to 2, which suggested a good overall stability as far as the release of free Gd³⁺ ions is concerned.

Uptake of Gd-DOTAMA-Gln and Gd-DOTAMA-C₆-Gln into Tumor Cells. The affinity of the two glutamine functionalized Gd complexes for different tumor cell lines has been determined and compared with that obtained with the nonspecific precursor Gd-DOTAMA-C₆-OH complex and the neutral Gd-HPDO3A (Prohance). To this purpose four tumor cell lines (HTC, rat hepatoma tissue culture; C6, rat glioma; TSA, murine breast adenocarcinoma; Neuro-2a, murine neuroblastoma) and healthy rat hepatocytes have been considered for the “in vitro” screening. The procedure used in this study consisted of incubating about 2–3 million cells for 6 h at 37 °C in a minimum medium (Earl’s balanced salt solution: EBSS) containing the Gd complexes at 1.6 mM (i.e., about 3 times larger than the glutamine physiological concentration). After incubation the cells were washed three times with ice-cold PBS and detached from the culture flasks mechanically with a cell scraper. Figure 1 shows the number of Gd moles taken up by the different cell lines as a function of the complex added to the incubation media. For all tumor cell lines, the number of moles of Gd found after the incubation with Gd-DOTAMA-C₆-Gln was more than 1×10^{-8} mol/mg of cell protein, whereas with the other compounds (Gd-DOTAMA-Gln, Gd-DOTAMA-C₆-OH, Gd-HPDO3A) the amounts of uptaken Gd were very low and just above the detection limit. Conversely, the amounts determined after the incubation in the primary culture of rat hepatocytes were very similar for all four compounds. The control (untreated) and the Gd labeled cell lines showed similar viability (95–98%) when tested with the trypan-blue methodology. To demonstrate that the glutamine residue present on the surface of the Gd-DOTAMA-C₆-Gln complex was the vehicle for the internalization through the amino acid transporting system, competition assays with free amino acid were carried out. Figure 2 shows that the uptake of the Gd-DOTAMA-C₆-Gln complex by HTC cells decreases markedly as the concentration of the free glutamine added to the culture medium increases. Interestingly, when the same competition assay is carried out with Gd-DOTAMA-Gln (Figure 2), no effect was observed. This result outlines the importance of the aliphatic chain (–C₅H₁₀–) introduced as a spacer between the DOTA coordination cage and the glutamine moiety. The spacer reduces the hindrance of the whole complex, improving the interaction of the glutamine moiety with the receptor on the cell membrane.

Scheme 2. Gd-DOTAMA-C₆-OH and Gd-DOTAMA-C₆-Gln Syntheses^a

^a (i) Bromoacetyl bromide, K₂CO₃, CH₃CN; (ii) DO3A-tris-*tert*-butyl ester, K₂CO₃, CH₃CN; (iii) H₂, 10% Pd/C, MeOH; (iv) CH₂Cl₂/TFA (1:1, v/v); (v) *N*-hydroxysuccinimide, EDC, CH₂Cl₂; (vi) L-glutamine, CH₃CN/phosphate buffer, (1:1, v/v), pH 8; (vii) CH₂Cl₂/TFA (1:1, v/v).

Table 1. Best-Fitting Parameters from Analyses

| complex | Δ^2 (s ⁻² /10 ¹⁹) | τ_v (ps) | τ_r (ps) | τ_M (μ s) | ΔH_m (kJ mol ⁻¹) | ΔH_v (kJ mol ⁻¹) |
|-------------------------------|--|----------------------|---------------------|------------------------|---|---|
| Gd-DOTAMA-C ₆ -OH | 1.4 ± 0.7 ^a | 40 ± 16 ^a | 70 ± 4 ^a | 1.3 ± 0.3 ^b | 19 ± 5 ^b | 40 ± 8 ^b |
| Gd-DOTAMA-Gln | 1.2 ± 0.8 ^a | 32 ± 5 ^a | 69 ± 5 ^a | 1.4 ± 0.4 ^b | 20 ± 4 ^b | 26 ± 5 ^b |
| Gd-DOTAMA-C ₆ -Gln | 1.5 ± 0.9 ^a | 25 ± 5 ^a | 83 ± 6 ^a | 1.3 ± 0.3 ^b | 26 ± 5 ^b | 32 ± 7 ^b |

^a Best-fitting parameters obtained from the analysis of the NMRD profile by considering one inner-sphere water molecule ($q = 1$) whose protons are at an average metal distance of 3 Å. ^b Best-fitting parameters obtained from the analysis of the ¹⁷O NMR profile by considering the temperature dependence of ¹⁷O-R_{2p} for an 18 mM solution of Gd-DOTAMA-Gln by using a Gd-¹⁷O scalar coupling constant of -3.8×10^6 rad s⁻¹ and a Gd-¹⁷O distance of 2.5 Å.

Further, relaxometric investigations allowed us to get more insights into the intracellular localization of Gd-DOTAMA-C₆-

Gln. Recently, we have shown³⁹ that when the uptake leads to a dispersion of the Gd chelate in the cytoplasm, the observed

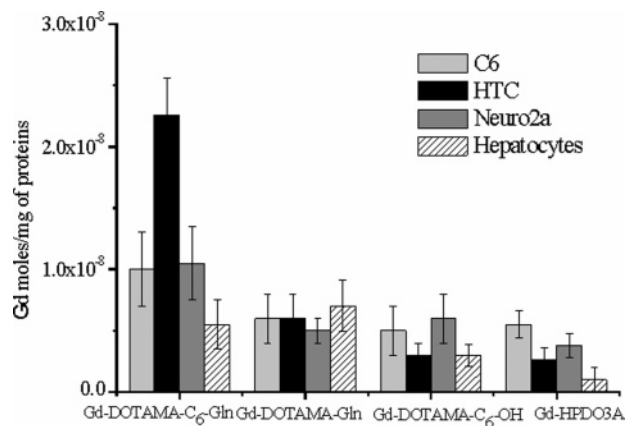


Figure 1. Internalization of Gd chelates in different cell types upon incubation for 6 h at 37 °C in the presence of 1.6 mM of the MR-imaging probes.

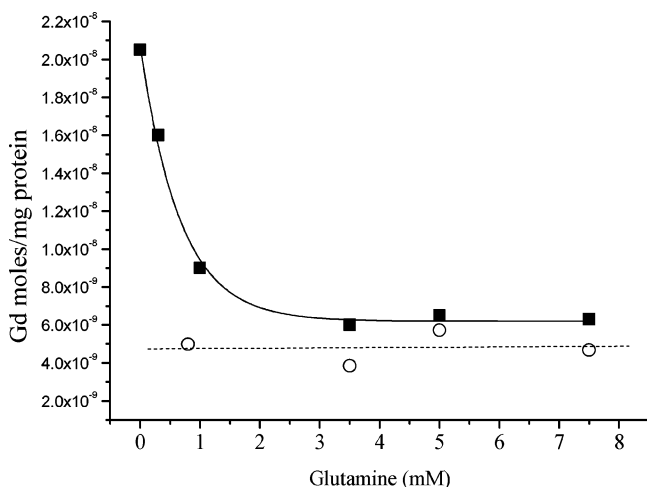


Figure 2. Effect of the addition of glutamine to the incubation medium on the amounts of internalized Gd-DOTAMA-C₆-Gln (■) and Gd-DOTAMA-Gln (○) into HTC cells.

water proton relaxation rate is directly proportional to the amount of the internalized Gd. Conversely, in the case of the entrapment in endosomes, a “quenching” effect in the relaxation enhancement takes place when the amount of uptaken Gd chelates is increased. This is due to the fact that the endosomal compartmentalization involves, for the water molecules, the crossing of an additional barrier to interact with the paramagnetic centers. Therefore, the measurements of the relaxation rate as a function of the internalized Gd provide us with the route to understanding whether the uptake of the Gd chelates takes the endosomal route or whether it leads to a dispersion in the cytoplasmatic compartment. Figure 3 reports the observed relaxation rates ($R_{1\text{obs}}$) vs the number of Gd³⁺ ions per cell. The relaxation rates were measured at 20 MHz and 25 °C on HTC incubated with Gd-DOTAMA-C₆-Gln for 6 h. Clearly the obtained plot is far from the calculated straight line (with a slope equal to the relaxivity of the complex measured in water), which indicates that the internalization occurred through the entrapment into endosomal vesicles.

On the basis of these results, the complex Gd-DOTAMA-C₆-Gln was considered for the following “in vitro” and “in vivo” MRI studies.

“In Vitro” MRI Experiments. To assess if the amount of internalized Gd is enough for the MRI visualization of tumor cells with respect to healthy ones, an “in vitro” MRI experiment was performed. For this purpose rat hepatocytes and HTC cells

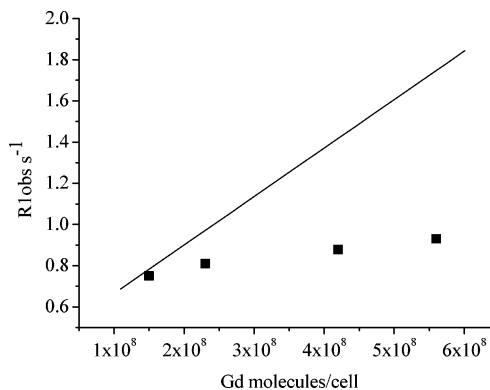


Figure 3. Observed proton relaxation rates ($R_{1\text{obs}}$), measured at 20 MHz and 25 °C, of HTC-cellular pellets ($\sim 5 \times 10^6$ cells) undergone to increased internalization of Gd-DOTAMA-C₆-Gln chelates. The straight line represents the calculated values that should have been observed if the relaxivity of Gd-DOTAMA-C₆-Gln was not “quenched” by the entrapment into endosomal vesicles.

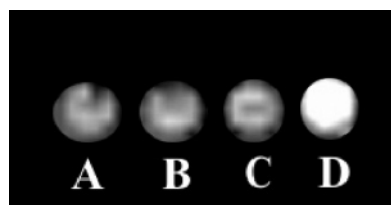


Figure 4. T_1 weighted spin-echo MR image (measured at 7 T), of an agar phantom containing unlabeled hepatocytes (A), hepatocytes labeled with Gd-DOTAMA-C₆-Gln (B), unlabeled HTC (C), and HTC labeled with Gd-DOTAMA-C₆-Gln (D).

were incubated for 4 h in the presence of the same amount (1.6 mM) of Gd-DOTAMA-C₆-Gln. Figure 4 shows that pelleted HTC cells, labeled with Gd-DOTAMA-C₆-Gln (23 nmol of Gd/mg of proteins), displayed a hyperintense signal on the T_1 weighted spin-echo image with respect to the unlabeled cells. This demonstrates the occurrence of an efficient uptake of the paramagnetic imaging probe. To the contrary, the signal intensity of the healthy rat hepatocytes is just above the signal intensity of the unlabeled cells. In fact, in this case the amount of Gd-DOTAMA-C₆-Gln internalized (5.5 nmol of Gd/mg of proteins) is about 4 times lower than that found on the hepatoma cells (HTC). As a consequence of the increased uptake of Gd-DOTAMA-C₆-Gln by tumor cells, there is about a 45% enhancement in the intensity of the rat hepatoma pellet when compared with the pellet of cells derived from the healthy rat liver.

“In Vivo” Targeting of Glutamine Receptors. To assess the “in vivo” capability of the complex Gd-DOTAMA-C₆-Gln to discriminate between tumor and normal tissues, a MRI study was carried out on two tumor bearing animal models: (1) A/J mice grafted with the murine neuroblastoma cell line Neuro-2a;⁴⁰ (2) Her-2/neu transgenic mice developing multiple mammary carcinomas after varying periods of latency.³³

The preparation of the first model was carried out by injecting 1 million Neuro-2a cells, subcutaneously, on the right limb of five male A/J mice. At 10–12 days after implantation, a tumoral mass of a 2–3 cm width is clearly detectable in each mouse at the site of injection. At this time, a first group of animals ($n = 4$) received intravenously 0.2 mmol/kg dose of the Gd-DOTAMA-C₆-Gln complex and a second group ($n = 3$) received the same dose of Gd-HPDO3A. Fat-suppressed T_1 weighted multislice multiecho MR images were recorded at 10 min, 20 min, 30 min, 24 h, and 72 h after the contrast

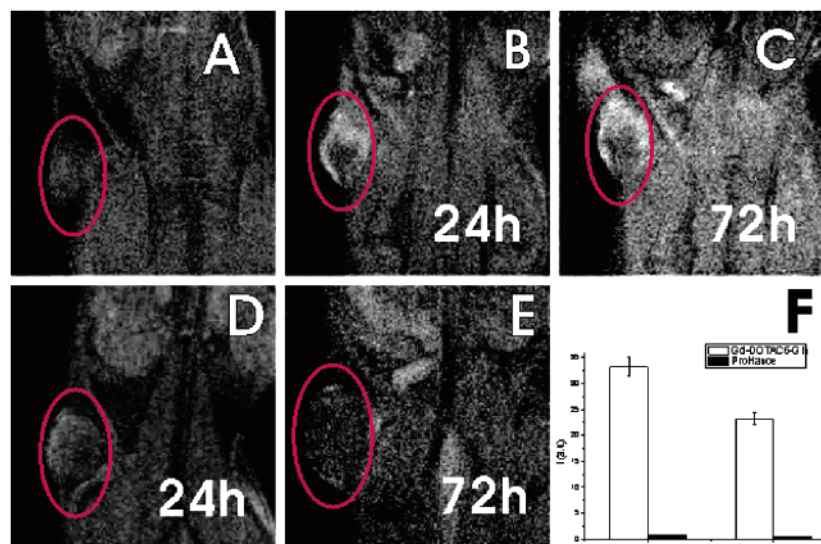


Figure 5. T_1 weighted spin-echo images of A/J mice grafted with the murine neuroblastoma cell line (Neuro-2a) recorded before (A) and after the administration of 0.2 mmol/kg of Gd-DOTAMA-C₆-Gln (B, C) and Gd-HPDO3A (D, E) at 24 and 72 h, respectively. (F) SI enhancement measured 24 and 72 h after the administration of the two contrast agents.

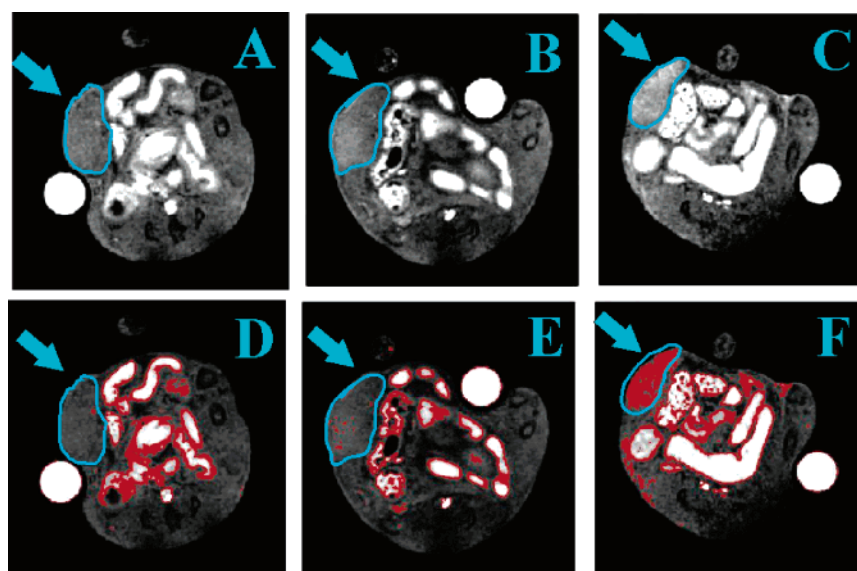


Figure 6. “In vivo” T_1 weighted spin-echo images of HER-2/neu tumors obtained before (A) and 72 h after the iv administration of 0.2 mmol/kg of Gd-HPDO3A (B) and Gd-DOTAMA-C₆-Gln (C). Arrows show the enhanced tumor regions. Images D–F are the same images printed using red color for pixels with a signal intensity value between 40 and 70 (on a scale of 1–100 in arbitrary units).

administration. The tumor images obtained a few minutes after the injection did not show any difference between the glutamine-containing compound and the nonspecific extracellular Gd-HPDO3A. Conversely, after 24 and 72 h, when the renal elimination of the noninternalized Gd complex was completed, the tumor SI enhancement of mice receiving Gd-DOTAMA-C₆-Gln was significantly higher (Figure 5). The amount of internalized Gd complex is large enough to yield a significant effect on the MRI signal intensity because of the decrease of the longitudinal relaxation time (T_1) in the tumor region. The signal enhancement is definitely higher in the tumor periphery. The histogram in Figure 5F shows the specific tumor SI enhancement compared with that observed after the administration of the same dose of Gd-HPDO3A.

Similar results have been obtained using cancer prone rat Her2/neu transgenic mice of 24 weeks of age. The first group of 13 mice received intravenously 0.2 mmol/kg of Gd-DOTAMA-C₆-Gln, while a second group of 10 mice received the same amount of Gd-HPDO3A as a negative control. All

mice developed at least one lobular carcinoma at their mammary glands; in some cases two or three tumors of different size could be detected on the same mouse. Fat-suppressed T_1 weighted multislice multiecho MR images were recorded at 10 min, 30 min, 24 h, and 72 h after the contrast administration. Analogous to what has been reported above, no significant difference was detected in the tumor region between the two contrast agents in the images recorded up to a few hours after their administration, whereas at 24 and 72 h the tumor SI was selectively enhanced in mice treated with Gd-DOTAMA-C₆-Gln (Figure 6). Interestingly, as shown in Figure 7, the SI enhancement is homogeneously distributed in the tumor mass and is more pronounced in tumors with a diameter less than 3 mm with respect to those with a larger diameter. No residual SI enhancement was observed in the neighboring tissue (e.g., muscle) 24 and 72 h after the administration of both contrast agents, whereas a 15% SI enhancement was detected on the kidney cortical region 24 and 72 h after the administration of Gd-DOTAMA-C₆-Gln.

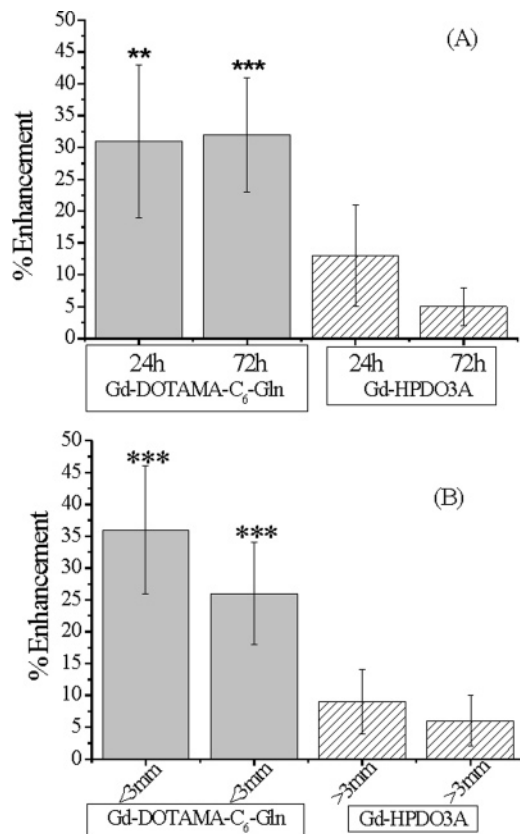


Figure 7. (A) Her-2/neu tumors SI enhancement measured 24 and 72 h after the administration of Gd-HPDO3A and Gd-DOTAMA-C₆-Gln. (B) Her-2/neu tumors SI enhancement measured 24 and 72 h after the administration of Gd-HPDO3A and Gd-DOTAMA-C₆-Gln displayed as a function of tumor mass (>3 mm and <3 mm).

Table 2. ICP-MS Determination of the Gd Amount Taken Up by Her-2/Neu Tumors^a

| | Gd amount taken up (nmol/g) | |
|--------------|-------------------------------|-------------|
| | Gd-DOTAMA-C ₆ -Gln | Gd-HPDO3A |
| tumor, <3 mm | 2.1 ± 0.4 | 0.33 ± 0.08 |
| tumor, >3 mm | 1.2 ± 0.4 | 0.18 ± 0.07 |
| muscle | 0.28 ± 0.06 | <0.05 |

^a Mice were sacrificed 24 h after the injection of the contrast agent (0.2 mmol/kg).

Quantitative Assessment of “in Vivo” Gadolinium Tumor Uptake by ICP-MS. The gadolinium amount taken up by Her-2/neu tumors was determined 24 h after the administration of the Gd-DOTAMA-C₆-Gln complex by inductively coupled plasma mass spectrometry (ICP-MS) and compared with that obtained with Gd-HPDO3A. The results summarized in Table 2 shows that the amount of Gd-DOTAMA-C₆-Gln taken up by tumors (expressed in nmol/g of tissue) is 7–8 times higher than that found in the neighboring tissue (muscle) for tumors less than 3 mm and 4 times for tumors greater than 3 mm. As observed in the MRI signal intensity analysis, the gadolinium amount taken up is more pronounced in small tumors with respect to those with a diameter greater than 3 mm. By use of the same ICP-MS protocol, the gadolinium amount accumulated in tumors 24 h after the administration of the same dose of Gd-HPDO3A was 6–7 times lower.

Discussion

The development of new agents that accumulate at the targeting site is an important task for molecular imaging applications. This objective has become crucial for MRI because

it is less sensitive with respect to other imaging modalities. In the present study, the visualization of tumor cells has been pursued exploiting the up-regulation of the glutamine transport system. In fact, transformed cells possess a highly efficient mechanism for the transport of glutamine, extracting large amounts of this amino acid from the blood “in vivo” and “in vitro” from cell culture media. For example, kinetic experiments found that in different hepatoma derived cells (SK-Hep, HepG2, Huh-7, H4, HTC) the glutamine transport rates were 10- to 30-fold higher ($K_m = 93\text{--}450 \mu\text{M}$; $V_{max} = 18\text{--}37$ (nmol/mg proteins)/min)^{29,41,42} than in normal hepatocytes ($K_m = 600\text{--}800 \mu\text{M}$; $V_{max} = 2.6\text{--}4.1$ (nmol/mg proteins)/min).^{29,42} Indicatively, the transport systems overexpressed on hepatoma cells should internalize 1–5000 million glutamine (molecules/cell)/min. For these reasons, we surmised that the targeting of these high-capacity carrier proteins could be an efficient route to the visualization of tumor cells. In principle, a much easier route to prepare Gd complexes bearing glutamine residues on their surfaces can be undertaken by the use of DTPA bis-anhydride that reacts promptly with amino groups to form the corresponding amide derivatives. Therefore, glutamine can be conjugated either directly (through the reaction of its amine group) or through a proper spacer (e.g., an ethylenediamine moiety). However DTPA mono- and bis-amide systems do not yield sufficiently stable Gd(III) chelates⁴³ and, in contact with cell membranes, an activated release of free Gd³⁺ ions takes place leading to a harmful uptake of Gd³⁺ ions from endogenous biological structures. On these grounds we abandoned any approach based on the use of DTPA-bis-anhydride in favor of the more labor demanding routes leading to probes based on Gd-DOTA chelates whose outstanding⁴ thermodynamic stability ensures against the release of Gd³⁺ ions. The “in vitro” studies on tumor cells (HTC, C6, TSA, Neuro-2a) showed that the complex Gd-DOTAMA-C₆-Gln is taken up by cells 2–7 times more efficiently than the other complexes investigated in this work. Interestingly, the different affinity for the Gd-DOTAMA-C₆-Gln complex shown by the examined cells derived from different tumors reflected the kinetic characteristics reported in the literature for similar cell lines.^{41–42,44–46}

Furthermore, the addition of increasing amounts of free glutamine to the culture medium markedly inhibits the cellular uptake. These observations help to prove that glutamine is the vehicle for the interaction of this complex with tumor cells. The different behavior shown by Gd-DOTAMA-Gln is likely a consequence of the hindrance of the Gd coordination cage directly bound to the amino acid. This limits the binding to the transporter protein on the cell membrane. To allow the interaction with the transporter on the cell membrane, it is necessary to introduce an aliphatic spacer between the glutamine moiety and the DOTA coordination cage.

Since the cells are particularly able to bind free Gd³⁺ ions,⁴³ it was very important to check the absence of any unchelated metal ions after the complexation step. It has been found that the occurrence of <0.3% of free Gd³⁺ represents an acceptable threshold because the amount eventually added to the incubation medium is such that it does not alter the conclusions drawn from the binding/uptake experiments. The attainment of such low values of unchelated Gd³⁺ ions is not a trivial task for systems such as those considered in this work that contain donor atoms on the surface of the ligand, thus offering potential coordination sites for unchelated Gd³⁺ ions. This finding calls for caution when systems containing longer peptide chains are considered. Another important point is whether the differential uptake of glutamine from tumor and benign cells could be

visualized by MRI. In fact, the amount of Gd-DOTAMA-C₆-Gln found in hepatoma cells was about 4 times higher than that found in normal hepatocytes. This amount of internalized complex produced a significant difference in signal intensity in the T₁ weighted image, which allows the “in vitro” discrimination between hepatoma and normal hepatocytes.

MRI detection of the glutamine uptake was then performed “in vivo” on two mice models (A/J mice grafted with murine neuroblastoma cells and Her-2/neu transgenic mice). The SI analysis of fat-suppressed T₁ weighted spin-echo images recorded 24 and 72 h after the CA administration showed the accumulation of the Gd-DOTAMA-C₆-Gln complex in tumors (both grafted and spontaneous) and in the kidneys (which with the gut are the main organs showing a net uptake of glutamine from the blood).⁴⁷ In contrast, the aspecific Gd-HPDO3A, administered at the same dose, was totally eliminated from the body. Interestingly, in Her-2/neu mice the SI enhancement was inversely proportional to the tumor diameter. In fact, tumors with a diameter less than 3 mm showed a higher SI enhancement than that measured on tumors with a diameter between 3 and 6 mm. This can be a consequence of a decreased accessibility of the intravenously injected CA to the tumor mass, due to the presence of a smaller number of microvessels per volume unit typical of these last stage tumors. In fact, this type of spontaneous carcinoma, once developed, no longer requires a profuse vascular supply.⁴⁸ The few vessels of the stroma of neoplastic lobular-alveolar structures are enough to sustain their relatively low rate of proliferation.

In summary, Gd-DOTAMA-C₆-Gln displays several positive features. The small size allows its easy extravasation and diffusion into the tissue to reach the surface of tumor cells. It is internalized by receptor-mediated endocytosis, thus avoiding harmful interactions with the molecules of the cytoplasm. It is easy to synthesize and has a long shelf life. The main drawback deals with the reduced recognition ability of the glutamine moiety on the chelate with respect to the free amino acid. In fact, the conjugation to the imaging reporter implied the transformation of an amino into an amide functionality, thus sacrificing one of the four glutamine recognition points on its transporting proteins. This drawback may be overcome by designing systems in which the conjugation step involves the aliphatic carbon backbone of the glutamine. Another interesting insight into obtaining a sensitivity enhancement for this class of glutamine transporter targeting agents relies on the observation that the internalization occurs through a receptor-mediated endocytosis. It is likely that upon binding of the modified glutamine residue, the transporting protein is unable to proceed with the successive steps that bring glutamine into the cytoplasm; thus, it moves to the clathrin-rich region to undergo its entrapment into the endosomal vesicles. On this basis, an increase in tumor visualization may be pursued by synthesizing systems containing two or even more Gd chelates as the payload of the glutamine carriers. Finally, it is worth noting that this work nicely parallels the recently reported results by Luciani et al.²⁵ who showed that MRI visualization of tumor cells can be achieved by targeting a glucose transporter whose up-regulation in neoplastic cells is analogous to that found in amino acid transporting systems. However, to carry enough imaging reporters at the target, they used liposomes loaded with Gd chelates, whose size limited the access only to glucose transporters on the endothelial walls of the tumoral tissue. Clearly, targeting glutamine transporters with small, stable Gd chelates appears to be a more efficient route for an improved delineation of the pathological tissue.

Experimental Section

¹H NMR and ¹³C NMR spectra were obtained on a Bruker Avance 300 (300 and 75 MHz respectively) spectrometer. Elemental analyses were performed with a Perkin-Elmer 240 apparatus.

The longitudinal water proton relaxation rate was measured on a Stellar Spinmaster spectrometer (Stellar, Mede, Italy) operating at 20 MHz, by means of the standard inversion-recovery technique (16 experiments, 2 scans). A typical 90° pulse width was 3.5 μs, and the reproducibility of the T₁ data was ±0.5%. The 1/T₁ nuclear magnetic relaxation dispersion profiles of water protons were measured over a continuum of magnetic field strength from 0.000 24 to 0.5 T (corresponding to 0.01–20 MHz proton Larmor frequency) on the fast field-cycling Stellar Spinmaster FFC 2000 relaxometer equipped with a silver magnet. The relaxometer operates under complete computer control with an absolute uncertainty in the 1/T₁ values of ±1%. The typical field sequences used were the NP sequence between 40 and 8 MHz and PP sequence between 8 and 0.01 MHz. The observation field was set at 13 MHz. Sixteen experiments of two scans were used for the T₁ determination for each field. Variable-temperature ¹⁷O NMR measurements were recorded on a JEOL EX-90 (2.1 T) spectrometer, equipped with a 5 mm probe, by using D₂O as the external lock. Experimental settings were as follows: spectral width 10 000 Hz, pulse width 7 μs, acquisition time 10 ms, 1000 scans, and no sample spinning. Solutions containing 2.6% of ¹⁷O isotope (Yeda, Israel) were used. The observed transverse relaxation rates (R_{2obs}^O) were calculated from the signal width at half-height.

Mass spectra were acquired using a XCT Plus electrospray ionization ion trap (ESI-IT) mass spectrometer (Agilent Italia, Milan, Italy). Analytical HPLC were acquired on an Agilent HP1100 equipped with a low-pressure quaternary pump and single-wavelength UV detector and on an Amersham AKTA Purifier 10/100 equipped with high-pressure binary pumps and three-wavelength UV detector. All starting materials were obtained from Sigma-Aldrich Co. and were used without further purification. Gd-HPDO3A (Prohance) was kindly provided by Bracco S.p.A. (Milano, Italy).

Syntheses of the Ligands. The DOTAMA-Gln ligand was synthesized according to a previously reported procedure.³⁴

Synthesis of 7-Aza-9-bromo-8-oxononanoic Acid Benzyl Ester (1). In a round-bottom flask, 6-aminohexanoic acid benzyl ester (71 g, 0.18 mol) and K₂CO₃ (49.90 g, 0.36 mol) were mixed in acetonitrile (1.1 L). The mixture was stirred at 0–5 °C for 1 h, then a solution of bromoacetyl bromide (15.75 mL, 0.18 mol in 200 mL of acetonitrile) was slowly dropped in 4 h. After another 40 min, the solid was removed and the organic phase was evaporated under reduced pressure. The residue was dissolved in dichloromethane (540 mL) and washed with a 5% solution of Na₂CO₃ (2 × 250 mL), with H₂O (250 mL), with 0.01 N HCl (2 × 250 mL), and finally again with water (250 mL). The organic phase was dried with sodium sulfate, filtered, and evaporated under reduced pressure. The residue corresponding to the product (2) was then dried under vacuum to achieve a white solid (123 g, yield 80%). ¹H NMR (CDCl₃) δ 7.35 (s, 5H, C₆H₅, 5H); 6.5 (broad, 1H, NH, 1H); 5.1 (s, 2H, C₆H₅CH₂, 2H); 3.82 (s, CH₂Br, 2H); 3.28 (m, CH₂NH, 2H); 2.36 (t, J = 7.2 Hz, CH₂COOBz, 2H); 1.70, 1.55, 1.35 (m, CH₂ aliphatic chain, 6H); ¹³C NMR (CDCl₃) δ 174.1, 165.6 (carboxyl and carboxamide groups, 2C); 136.2, 128.8, 128.4 (C₆H₅, 6C); 66.42 (C₆H₅CH₂, 1C); 40.16 (CH₂Br, 1C); 34.27, 29.56, 29.14, 26.46, 24.65 (CH₂ aliphatic chain, 5C); HPLC method 1 (Supporting Information) (CL003), retention time 22.5 min, purity >90%.

Synthesis of 1-(3-Aza-8-carboxy-2-oxooctyl)-4,7,10-tris((1,1-dimethylethoxy)carbonylmethyl)-1,4,7,10-tetraazacyclododecane Benzyl Ester (2). DO3A-tris-*tert*-butylester⁴⁹ (51.44 g, 0.1 mol) was dissolved in acetonitrile (1.25 L), and solid K₂CO₃ (16.58 g, 0.12 mol) was added. The mixture was stirred at 0–5 °C, and a solution of 1 (36.76 g, 0.107 mol in 350 mL of acetonitrile) was slowly dropped over a period of 5 h. The reaction mixture was left stirring for another hour. After filtration the solvent was removed

by evaporation under reduced pressure, and the residue was treated with diethyl ether (150 mL) to give a white solid. After filtration, the solution was evaporated in a vacuum and the desired product was collected as a colorless oil (75 g, yield 96.5%). The product spontaneously loses the benzyl moiety; therefore, it was directly used in the next step without further purification and characterization. HPLC method 1 (Supporting Information), retention time 16.17 min, purity 84%.

Synthesis of 1-(3-Aza-8-carboxy-2-oxooctyl)-4,7,10-tris((1,1-dimethylethoxy)carbonylmethyl)-1,4,7,10-tetraazacyclododecane-DOTAMA(*t*BuO)₃-C₆-OH (3). Product 2 (75 g) was dissolved in methanol (100 mL), and 7 g of 10% Pd/C was added. Then the reaction was carried out under hydrogen at atmospheric pressure and room temperature for 4 h.

The mixture was then filtered, and the solvent was evaporated. The solid obtained was dissolved in CH₂Cl₂/MeOH, 15:1 v/v (150 mL), and purified by flash chromatography on a 7.5 cm × 30 cm silica column with the same elution mixture. After solvent evaporation 33 g of a white solid was obtained (yield 50%). ¹H NMR (DMSO) δ 8.26 (t, *J* = 6.0 Hz, CONH, 1H); 3.05 (m, CONHCH₂, 2H); 2.20 (t, *J* = 7.2 Hz, CH₂COOH, 2H); 3.7–2.4, 2.4–1.8 (broad signals, CH₂ ring and NCH₂CO, 24H); 1.47, 1.45 (s, C(CH₃), 27H); 1.48 (m, CH₂ aliphatic chain, 4H); 1.25 (tt, *J* = 7.2 Hz, CH₂ aliphatic chain, 2H); ¹³C NMR (CD₃OD) δ 176.56, 173.28, 172.94, 172.01 (carboxyl and carboxamide groups, 4C); 81.52 (C(CH₃)₃, 3C); 56.20, 55.64 (NCH₂CO, 4C); 53–47 (broad signals, NCH₂ ring, 8C); 24.86, 26.52, 29.37, 34.17, 38.98 (CH₂ aliphatic chain, 5C); 27.29–27.38 (C(CH₃)₃, 9C); ESI-MS *m/z* calculated 685.46 (M), found 686.38 (MH⁺).

Synthesis of 1-(3-Aza-8-carboxy-2-oxooctyl)-4,7,10-tris(carboxymethyl)-1,4,7,10-tetraazacyclododecane (4)-DOTAMA-C₆-OH. To a solution of 3 (2.0 g, 2.91 mmol) in dichloromethane (40 mL), cooled in an ice bath, was slowly added neat trifluoroacetic acid (1.35 mL, 17.5 mmol). The solution was stirred for 1 h at room temperature. The dichloromethane was evaporated, and the residue was treated with trifluoroacetic acid (10 mL, 130 mmol) and triisopropylsilane (0.3 mL). The solution was stirred for 48 h. Then diethyl ether (20 mL) was slowly added to give a white solid, which was filtered and washed with ether (5 × 30 mL). The solid was redissolved in trifluoroacetic acid (10 mL) and left to stir for 72 h. Then diethyl ether (30 mL) was added to give a solid that was filtered, washed with ether (5 × 30 mL), and dried (in a vacuum and over P₂O₅ and NaOH). ¹H NMR (D₂O) δ 4.10–3.55 (broad signals NCH₂CO, 8H); 3.55–2.90 (broad signals, CH₂ ring and CONHCH₂, 18H); 2.95 (t, *J* = 7.2 Hz, CH₂CONH, 2H); 1.60, 1.53, 1.36 (m, CH₂ aliphatic chain, 6H); ¹³C NMR (D₂O) δ 176.38, 174.35, 173.56, 171.04 (carboxyl and carboxamide groups, 4C); 55.51, 54.79, 53.40 (NCH₂CO, 4C); 52.8 and 50.42 (NCH₂ ring, 8C); 39.25, 33.63, 29.01, 26.23, 24.35 (CH₂ aliphatic chain, 5C); HPLC method 2 (Supporting Information), retention time 22.01 min, purity 93%; ESI-MS *m/z* calculated 517.27 (M), found 518.19 (MH⁺). Anal. (C₂₂H₃₉N₅O₉·2CF₃COOH) C, H, N.

Synthesis of 1-(3-Aza-8-carboxy-2-oxooctyl)-4,7,10-tris((1,1-dimethylethoxy)carbonylmethyl)-1,4,7,10-tetraazacyclododecane *N*-Hydroxysuccinimide Ester-DOTAMA-C₆-NHS (5). A suspension of DOTAMA(*t*BuO)₃-C₆-OH (3) (11 g, 16 mmol) and of *N*-hydroxysuccinimide (2.72 g, 23 mmol) in CH₂Cl₂ (80 mL) was cooled to 0 °C and a solution of EDC (4.5 g, 23.5 mmol) in CH₂Cl₂ (80 mL) was added in 30 min. The mixture was stirred for 20 h at room temperature, washed with water (3 × 15 mL), and dried, and then the solvent was removed under vacuum to yield a pale-yellow oil, which was dried under reduced pressure and used without further purifications.

Synthesis of 1-(11-*S*)-3,10-Diaza-13-carboxamido-11-carboxy-2,9-dioxotridecyl)-4,7,10-tris((1,1-dimethylethoxy)carbonylmethyl)-1,4,7,10-tetraazacyclododecane (6). To a solution of L-glutamine (3 g, 20 mmol) in phosphate buffer (0.1M pH 8, 100 mL) and acetonitrile (200 mL) was slowly added, at room temperature, a solution of 5 in acetonitrile (50 mL). The mixture was allowed to stir for 24 h. Then the acetonitrile was removed by a reduced pressure evaporation and the aqueous phase was washed with

dichloromethane (3 × 100 mL). The organic phase was dried under sodium sulfate, and the solvent was evaporated to give a yellow solid (10.20 g). The solid was then purified by flash chromatography, was dissolved in a mixture of dichloromethane/methanol, 10:1, and loaded onto a silica column (5 cm × 20 cm). The sample was eluted with a gradient of methanol in dichloromethane (dichloromethane/methanol, volume): 10/1, 2000 mL; 9/1, 900 mL; 8/2, 1000 mL; 7/3, 1300 mL; 5/5, 800 mL). The fractions between 1200 and 5500 mL containing the desired product were collected and combined, and the solvent was removed to give a white solid (5.85 g, yield 48%). ¹H NMR (CDCl₃) δ 8.39 (t, *J* = 6 Hz, CONHCH₂, 1H); 8.07, 7.24 (s, CONH₂, 2H); 5.42 (s, CONHCH, 1H); 4.25 (m, CONHCH, 1H); 3.5–2.4, 2.4–2.2 (broad signals, CH₂ ring and NCH₂CO, 24H); 2.31 (m, CH₂CONH₂, 2H); 2.20 (m, CH₂CONH, 2H); 2.01 (m, CHCH₂CH₂CONH₂, 2H); 1.60, 1.48, 1.33 (m, CH₂ aliphatic chain, 6H); 1.41, 1.40 (s, C(CH₃), 27H); ¹³C NMR (CDCl₃) δ 176.95, 175.39, 172.87, 172.61, 172.32, 171.92 (carboxyl and carboxamide groups, 6C); 82.11, 82.00 (C(CH₃)₃, 3C); 56.34, 55.99, 55.83 (NCH₂CO, 4C); 54.59 (NHCHCOOH, 1C); 53.5–47.0 (broad signals, NCH₂ ring, 8C); 38.91, 36.60, 33.29, 30.38, 28.59, 25.88, 25.26 (CH₂ aliphatic chain and CH₂ glutamine moiety, 7C); 28.25, 28.19 (C(CH₃)₃, 9C); ESI-MS *m/z* calculated 813.52 (M), found 814.28 (MH⁺).

Synthesis of 1-(11-*S*)-3,10-Diaza-13-carboxamido-11-carboxy-2,9-dioxotridecyl)-4,7,10-tris(carboxymethyl)-1,4,7,10-tetraazacyclododecane (7)-DOTAMA-C₆-Gln. To a solution of 6 (5.86 g, 7 mmol) in dichloromethane (20 mL), cooled in an ice bath, was slowly added neat trifluoroacetic acid (3.30 mL, 42 mmol). The solution was stirred for 1 h at room temperature. The dichloromethane was evaporated, and the residue was treated with trifluoroacetic acid (16.20 mL, 210 mmol) and triisopropylsilane (0.5 mL). The solution was stirred for 48 h, then diethyl ether (30 mL) was slowly added to give a white solid, which was filtered and washed with ether (5 × 30 mL). The solid was redissolved in trifluoroacetic acid (30 mL) and left to stir for 72 h. Then diethyl ether (150 mL) was added to give a solid, which was filtered, washed with ether (5 × 30 mL), and dried (in a vacuum and over P₂O₅ and NaOH). ¹H NMR (D₂O) δ 4.32 (dd, *J* = 5.1 Hz and *J* = 4.2 Hz, CONHCH, 1H); 4.2–3.8 and 3.8–3.55 (broad signals NCH₂CO, 8H); 3.5–3.25, 3.25–2.95 (broad signals, CH₂ ring and CONHCH₂, 18H); 2.34 (t, *J* = 7.2 Hz, CH₂CONH₂, 2H); 2.26 (t, *J* = 7.2 Hz, CH₂CONH, 2H); 2.12 and 1.96 (m, CHCH₂CH₂CONH₂, 2H); 1.56, 1.48, 1.28 (m, CH₂ aliphatic chain, 6H); ¹³C NMR (D₂O) δ 180.01, 179.25, 177.15, 175.48, 171.67, 167.52 (carboxyl and carboxamide groups, 6C); 57.15, 56.41, 55.30 (NCH₂CO, 4C); 54.24 (NHCHCOOH, 1C); 53.13 and 50.79 (NCH₂ ring, 8C); 41.47, 37.33, 33.34, 30.01, 28.48, 27.61, 26.90 (CH₂ aliphatic chain and CH₂ glutamine moiety, 7C); HPLC method 2 (Supporting Information), retention time 21.00 min, purity 90%; ESI-MS *m/z* calculated 645.33, found 646.43 (MH⁺). Anal. (C₂₇H₄₇N₇O₁₁·2CF₃COOH) C, H, N.

Synthesis of the Gd(III) Complexes. An equimolar amount of GdCl₃ solution (about 120 mM in water) was slowly added to a 40 mM ligand solution, maintaining the pH value at 6.5 with NaOH. The mixture was allowed to stir overnight at room temp, and then the pH was raised to 8.5 and the mixture was stirred for 2 h. Centrifugation at 7000 rpm for 5 min at 10 °C allowed the separation of Gd(OH)₃ from the solution. The amount of residual free Gd³⁺ ion was assessed by the orange xylenol UV method;³⁵ the overall Gd contents was determined by ¹H NMR *T*₁ measurement of the mineralized complex solution (in 6 M HCl at 120 °C for 16 h). When the amount of residual free Gd³⁺ ion was higher than 0.3% (mol/mol), a corresponding amount of ligand was added and allowed to react overnight. The procedure was repeated until the free Gd³⁺ ion was below 0.3%. The solution was then lyophilized to give a white solid. Characterization of Gd-DOTAMA-C₆-Gln: ESI-MS *m/z* calculated 800.23, found 799.3, 801.3 (MH⁺), more intense signals, isotopic distribution consistent with Gd complex; HPLC method 3 (see Supporting Information), retention time 16.2 min, purity 95%. Gd(III) free ion: 0.1% (by UV orange xylenol method). Anal. (C₂₇H₄₃N₇NaO₁₁·2CF₃COONa) C, H, N.

Cell Culture. The culture media DMEM F-12, DMEM, M199, and foetal bovine serum (FBS) were purchased from Cambrex, East Rutherford, NJ. The penicillin–streptomycin mixture, serum bovine albumin (BSA), trypsin, glutamine, and all other chemicals were from Sigma Chemical Co., St. Louis, MO. Rat tail tendon collagen was prepared as described by Strom and Michalopoulos.⁵⁰ Male Wistar rats weighing 150–200 g were used to isolate hepatocytes by the collagenase perfusion method.⁵¹ Their care was in accordance with the national guidelines for animal experimentation. The cells were plated at a density of 7×10^4 viable cells/cm² on culture dishes (10 cm diameter) coated with rat tail tendon collagen in M199 medium supplemented with 2 mg/mL BSA, 3.6 mg/mL HEPES, 100 U/mL penicillin, 100 μ g/mL streptomycin, 5% fetal bovine serum (FBS), and 1 nmol/L insulin and incubated in a humidified incubator with a CO₂/air atmosphere (5:95 v/v) at 37 °C. Only cell suspensions with a viability (tested by trypan-blue exclusion) of 70% or more were used. Four hours after cell seeding, the M199 medium was changed to fresh M199 supplemented with 10 nmol/L insulin instead of FBS, and the cells were incubated as described above. Cells were used for the uptake experiments after 24 h of culture. All other cells were cultured in 75 cm² flasks in a humidified incubator at 37 °C and at CO₂/air (5:95 v/v).

C6 (rat glioma cell line) and HTC (rat hepatoma tissue culture) were grown in DMEM F-12 medium supplemented with 5% FBS, 2 mM glutamine, 100 U/mL penicillin, and 100 μ g/mL streptomycin. TSA murine breast adenocarcinoma and Neuro-2a murine neuroblastoma were grown in DMEM medium supplemented with 10% FBS, 2 mM glutamine, 100 U/mL penicillin, and 100 μ g/mL streptomycin. For the uptake experiments, C6 and TSA cells were seeded in 10 cm Petri dishes at a density of 4×10^4 cells/cm². Neuro-2a and HTC cells were seeded at a density of 2.5×10^4 and 1.5×10^4 cells/cm². Twenty-four hours after seeding, cells were ready for the uptake experiments.

Uptake Experiments. C6, HTC, TSA, Neuro-2a, and rat hepatocytes seeded in 10 cm diameter culture dishes were used to carry out the uptake experiments with the gadolinium complexes. After removal of the culture medium, cells were washed with 5 mL of phosphate saline buffer (PBS), and then an amount of 5 mL of Earl's balanced salt solution (EBSS: CaCl₂ 0.266 g/L; KCl 0.4 g/L; NaCl 6.8 g/L; glucose 1 g/L; MgSO₄ 0.204 g/L; NaH₂PO₄ 0.144 g/L; NaHCO₃ 1.1 g/L; pH 7.4) was added. Cells were incubated for 6 h with the different compounds at 37 °C and in CO₂/air (5:95 v/v). At the end of the incubation, the medium was removed and cells were washed three times with ice-cold PBS. Then cells were recovered from the Petri dishes in 250 μ L of PBS with a cell scraper. The Gd³⁺ concentration in each pellet was determined as described previously.⁵² Any value obtained is the average of three different experiments. Protein concentration of each sample was determined from cell lysates by the Bradford method⁵³ using bovine serum albumin as standard.

Determination of Intracellular Relaxivity. In each experiment, about 5–6 million cells were incubated at 37 °C for 6 h in EBSS containing increasing amounts of Gd-DOTAMA-C₆-Gln (from 0.8 to 2.5 mM). After this treatment, the cells were washed three times with 10 mL of ice-cold PBS, detached with trypsin/EDTA, and transferred into a 5 mm NMR tube. The tubes containing the cell suspensions were placed in a centrifuge at 1000g for 5 min. The supernatant was carefully removed, and the T₁ of the cellular pellets was measured at 0.5 T and 25 °C on a Stellar Spinmaster spectrometer (Stellar, Mede, Italy) by means of the inversion–recovery pulse sequence. The Gd³⁺ concentration in each pellet was determined as described above.

Cell Viability Test. The trypan-blue exclusion test was used to assess cell viability. An aliquot (10 μ L) of each cell suspension, both control and treated cells, was well mixed with an equal amount of 0.4% trypan blue solution in PBS. An amount of 10 μ L of the solution was introduced in a counting chamber (hemocytometer). Viable cells were round and bright, while damaged cells appeared deep-blue because of the incorporation of the trypan dye. Viability was expressed in % (ratio of viable cells to total cells \times 100).

Animal Models. In vivo experiments were performed on A/J mice grafted with a murine neuroblastoma cell line and Her-2/neu animal models. Neuroblastoma transplantable tumors were obtained by subcutaneous injection of 1 million Neuro-2a cells on the right limb. Solid tumors of about 2–3 cm diameter formed in about 10–12 days were used for imaging evaluation.

Her-2/neu transgenic mice develop mammary carcinomas at a high multiplicity (all mammary glands are affected) and a relatively short latency (about 4 months) as a consequence of a point mutation at position 664 in the transmembrane domain of rat Her-2/neu oncogene (p185neu). In 3-week-old Her-2/neu mice, rat p185neu is markedly overexpressed on the surface of the cells of the rudimentary mammary gland. At 6 weeks, the rat p185neu cells give rise to a widespread atypical hyperplasia of small lobular ducts and lobules. Foci of “in situ” carcinoma first apparent around the 15th week evolve into invasive lobular carcinomas by the 20th week. Ten weeks later invasive lobular carcinoma is present in all the glands. Mice at 24 weeks of age were considered suitable for MRI experiments. Mice were constantly treated properly and humanely in accordance with European Community guidelines.

MRI. “In vitro” MR images of cell pellets were acquired on a Bruker Pharmascan 300 (7T) having actively shielded gradients (300 mT/m) and running ParaVision 3.2.2 software (Bruker Medical, Ettlingen, Germany) equipped with two birdcage resonators with 60 and 38 mm inner diameters, respectively. Five million of HTC and rat hepatocyte cells have been incubated for 4 h with the same amount (1.6 mM) of Gd-DOTAMA-C₆-Gln. After the incubation the cells were extensively washed with ice-cold PBS and collected in glass capillaries. Successively the capillary-containing cells were placed in an agar phantom for the MRI experiments. “In vivo” MR images of A/J mice grafted with Neuro-2a were acquired on the Bruker Pharmascan 300 (7T) described above. Prior to MRI examination animals were anesthetized by injecting tiletamine/zolazepam (Zoletil 100), 20 mg/kg, + xylazine (Rompun), 5 mg/kg. Mice of group 1 ($n = 5$) received intravenously 0.2 mmol/kg of Gd-DOTAMA-C₆-Gln, and mice of group 2 ($n = 3$) received the same amount of Gd-HPDO3A. MR images were acquired before and 10 min, 30 min, 24 h, and 72 h after the contrast administration using a T₁-weighted, fat-suppressed, multislice multiecho protocol (TR/TE/NEX 150/10/2, 1 slice, 1.5 mm). MR images of Her2/neu transgenic mice of 24 weeks of age were acquired on a Bruker Avance 300 (7T) equipped with a microimaging probe. The system is endowed with two birdcage resonators with 30 and 10 mm inner diameters, respectively. The animals were anesthetized as described above. Mice of group 1 ($n = 13$) received intravenously 0.2 mmol/kg of Gd-DOTAMA-C₆-Gln, and mice of group 2 ($n = 10$) received the same amount of Gd-HPDO3A. MR images were acquired before and 10 min, 30 min, 24 h, and 72 h after the contrast administration using a T₁-weighted, fat-suppressed, multislice multiecho protocol (TR/TE/NEX 200/3.2/6, 1 slice, 1 mm). Fat suppression was performed by applying a presaturation pulse (90° BW = 1400 Hz) at the absorption frequency of fat (–1100 Hz from water). The mean signal intensity (SI) values were calculated (a) on the whole tumor, (b) on a 4–5 mm² ROI drawn on the back tissue, and (c) on medullary and cortical regions of kidneys. For statistical analysis, one-way Student's *t* test was used. Probability values less than 0.05 were considered statistically different.

ICP-MS. Twenty-four hours after the administration of Gd-DOTAMA-C₆-Gln and Gd-HPDO3A, Her-2/neu mice ($n = 4$) were sacrificed and excised tissues were digested with 2 mL of concentrated HNO₃ (70%) under microwave heating (Milestone MicroSYNTH microwave labstation equipped with an optical fiber temperature control and HPR-1000/6M six-position high-pressure reactor, Bergamo, Italy). After digestion the volume of each sample was made up with 2 mL of ultrapure water and analyzed by ICP-MS (ICP-MS, Element-2, Thermo-Finnigan, Rodano (MI), Italy).

Acknowledgment. This work was supported by MIUR (PRIN and FIRB projects) and was carried out under the frame of COST D18 Action, EMIL, and DiMI EU NoEs. Support from Bracco Imaging SpA is gratefully acknowledged.

Supporting Information Available: Elemental analysis results for all target compounds and description of HPLC methods 1–3 used for the purification of intermediates and final products. This material is available free of charge via the Internet at <http://pubs.acs.org>.

References

- Rinck, P. A. *Magnetic Resonance in Medicine*; Blackwell Scientific Publications: Oxford, U.K., 1993.
- Merbach, A. E.; Toth, E. *The Chemistry of Contrast Agents in Medical Magnetic Resonance Imaging*; John Wiley & Sons: Chichester, U.K., 2001.
- Aime, S.; Botta, M.; Terreno, E. Gd(III)-based contrast agents for MRI. *Adv. Inorg. Chem.* **2005**, *57*, 173–237.
- Caravan, P.; Ellison, J. J.; McCurry, T. J.; Lauffer, R. B. Gadolinium-(III) chelates as MRI contrast agents: structure, dynamics and applications. *Chem. Rev.* **1999**, *99*, 2293–2352.
- Liu, S. The role of coordination chemistry in the development of target-specific radiopharmaceuticals. *Chem. Soc. Rev.* **2004**, *33*, 445–461.
- Fichna, J.; Janecka, A. Synthesis of target-specific radiolabeled peptides for diagnostic imaging. *Bioconjugate Chem.* **2003**, *14*, 3–17.
- Weiner, R. E.; Thakur, M. L. Radiolabeled peptides in the diagnosis and therapy of oncological diseases. *Appl. Radiat. Isot.* **2002**, *57*, 749–763.
- Nunn, A. D.; Linder, K. E.; Tweedle, M. F. Can receptors be imaged with MRI agents? *Q. J. Nucl. Med.* **1997**, *41*, 155–162.
- Aime, S.; Cabella, C.; Colombatto, S.; Geninatti Crich, S.; Gianolio, E.; Maggioni, F. Insights into the use of paramagnetic Gd(III) complexes in MR-molecular imaging investigations. *J. Magn. Reson. Imaging* **2002**, *16*, 394–406.
- Schmieder, A. H.; Winter, P. M.; Caruthers, S. D.; Harris, T. D.; Williams, T. A.; Allen, J. S.; Lacy, E. K.; Zhang, H.; Scott, M. J.; Hu, G.; Robertson, J. D.; Wickline, S. A.; Lanza, G. M. Molecular MR imaging of melanoma angiogenesis with alphavbeta3-targeted paramagnetic nanoparticles. *Magn. Reson. Med.* **2005**, *53*, 621–627.
- Winter, P. M.; Caruthers, S. D.; Kassner, A.; Harris, T. D.; Chinen, L. K.; Allen, J. S.; Lacy, E. K.; Zhang, H.; Robertson, J. D.; Wickline, S. A.; Lanza, G. M. Molecular imaging of angiogenesis in nascent Vx-2 rabbit tumors using a novel alphavbeta3-targeted nanoparticle and 1.5 T magnetic resonance imaging. *Cancer Res.* **2003**, *63*, 5838–5843.
- Anderson, S. A.; Rader, R. K.; Westlin, W. F.; Null, C.; Jackson, D.; Lanza, G. M.; Wickline, S. A.; Kotyk, J. J. Magnetic resonance contrast enhancement of neovasculation with alpha(v)beta(3)-targeted nanoparticles. *Magn Reson Med.* **2000**, *44*, 433–439.
- Sipkins, D. A.; Cheresch, D. A.; Kazemi, M. R.; Nevin, L. M.; Bednarski, M. D.; Li, K. C. Detection of tumor angiogenesis in vivo by alphaVbeta3-targeted magnetic resonance imaging. *Nat Med.* **1998**, *4*, 623–626.
- Funovics, M. A.; Kapeller, B.; Hoeller, C.; Su, H. S.; Kunstfeld, R.; Puig, S.; Macfelda, K. MR imaging of the her2/neu and 9.2.27 tumor antigens using immunospecific contrast agents. *Magn. Reson. Imaging* **2004**, *22*, 843–850.
- Artemov, D.; Mori, N.; Okollie, B.; Bhujwala, Z. M. MR molecular imaging of the Her-2/neu receptor in breast cancer cells using targeted iron oxide nanoparticles. *Magn. Reson. Med.* **2003**, *49*, 403–408.
- Artemov, D.; Mori, N.; Ravi, R.; Bhujwala, Z. M. Magnetic resonance molecular imaging of the HER-2/neu receptor. *Cancer Res.* **2003**, *63*, 2723–2727.
- Mulder, W. J.; Strijkers, G. J.; Griffioen, A. W.; van Bloois, L.; Molema, G.; Storm, G.; Koning, G. A.; Nicolay, K. A liposomal system for contrast-enhanced magnetic resonance imaging of molecular targets. *Bioconjugate Chem.* **2004**, *15*, 799–806.
- Warburg, O. On the origin of cancer cells. *Science* **1956**, *123*, 309–314.
- Couturier, O.; Luxen, A.; Chatal, J. F.; Vuillez, J. P.; Rigo, P.; Hustinx, R. Fluorinated tracers for imaging cancer with positron emission tomography. *Eur. J. Nucl. Med. Mol. Imaging* **2004**, *31*, 1182–1206.
- Kubota, K. From tumor biology to clinical PET: a review of positron emission tomography (PET) in oncology. *Ann. Nucl. Med.* **2001**, *15*, 471–486.
- Sammick, S.; Schaefer, A.; Siebert, S.; Richter, S.; Vollmar, B.; Kirsch, C. M. Preparation and investigation of tumor affinity, uptake kinetic and transport mechanism of iodine-123-labelled amino acid derivatives in human pancreatic carcinoma and glioblastoma cells. *Nucl. Med. Biol.* **2001**, *28*, 13–23.
- Conti, P. S. Introduction to imaging brain tumor metabolism with positron emission tomography (PET). *Cancer Invest.* **1995**, *13*, 244–259.
- Saris, S. C.; Solares, G. R.; Wazer, D. E.; Cano, G.; Kerley, S. E.; Joyce, M. A.; Adelman, L. S.; Harling, O. K.; Madoc-Jones, H.; Zamenhof, R. G. Boron neutron capture therapy for murine malignant gliomas. *Cancer Res.* **1992**, *52*, 4672–4677.
- Barth, R. F.; Coderre, J. A.; Vicente, M. G.; Blue, T. E. Boron neutron capture therapy of cancer: current status and future prospects. *Clin. Cancer Res.* **2005**, *11*, 3987–4002.
- Luciani, A.; Olivier, J. C.; Clement, O.; Siauve, N.; Brillet, P. Y.; Bessoud, B.; Gazeau, F.; Uchegbu, I. F.; Kahn, E.; Fria, G.; Cuenod, C. A. Glucose-receptor MR imaging of tumors: study in mice with PEGylated paramagnetic niosomes. *Radiology* **2004**, *231*, 135–142.
- Bode, B. P. Recent molecular advances in mammalian glutamine transport. *J. Nutr.* **2001**, *131*, 2475S–2485S.
- Souba, W. W. Glutamine and cancer. *Ann. Surg.* **1993**, *218*, 715–728.
- Medina, M. A. Glutamine and cancer. *J. Nutr.* **2001**, *131*, 2539S–2542S.
- Bode, B. P.; Kaminski, D. L.; Souba, W. W.; Li, A. P. Glutamine transport in isolated human hepatocytes and transformed liver cells. *Hepatology* **1995**, *21*, 511–520.
- Fischer, C. P.; Bode, B. P.; Souba, W. W. Adaptive alterations in cellular metabolism with malignant transformation. *Ann Surg.* **1998**, *227*, 627–634.
- Medina, M. A.; Sanchez-Jimenez, F.; Marquez, J.; Rodriguez Quesada, A.; Nunez de Castro, I. Relevance of glutamine metabolism to tumor cell growth. *Mol. Cell. Biochem.* **1992**, *113*, 1–15.
- Sidoryk, M.; Matyja, E.; Dybel, A.; Zielinska, M.; Bogucki, J.; Jaskolski, D. J.; Liberski, P. P.; Kowalczyk, P.; Albrecht, J. Increased expression of a glutamine transporter SNAT3 is a marker of malignant gliomas. *NeuroReport* **2004**, *15*, 575–578.
- Boggi, K.; Nicoletti, G.; Di Carlo, E.; Cavallo, F.; Landuzzi, L.; Melani, C.; Giovarelli, M.; Rossi, I.; Nanni, P.; De Giovanni, C.; Bouchard, P.; Wolf, S.; Modesti, A.; Musiani, P.; Lollini, P. L.; Colombo, M. P.; Forni, G. Interleukin 12-mediated prevention of spontaneous mammary adenocarcinomas in two lines of Her-2/neu transgenic mice. *J. Exp. Med.* **1998**, *3*, 188, 589–596.
- Lattuada, L.; Demattio, S.; Vincenzi, V.; Cabella, C.; Visigalli, M.; Aime, S.; Barge, A.; Geninatti Crich, S.; Gianolio, E. *Bioorg. Med. Chem. Lett.* **2006**, *16*(15), 4111–4. Epub 2006 May 18.
- Geninatti Crich, S.; Lanzardo, S.; Barge, A.; Esposito, G.; Tei, L.; Forni, G.; Aime, S. Visualization through magnetic resonance imaging of DNA internalized following “in vivo” electroporation. *Mol. Imaging* **2005**, *4*, 7–17.
- Powell, D. H.; Ni Dhubghaill, O. M.; Pubanz, D.; Helm, L.; Lebedev, Y.; Schlaepfer, W.; Merbach, A. E. Structural and dynamic parameters obtained from 170 NMR, EPR, and NMRD studies of monomeric and dimeric Gd³⁺ complexes of interest in magnetic resonance imaging: an integrated and theoretically self-consistent approach. *J. Am. Chem. Soc.* **1996**, *118*, 9333–9346.
- Banci, L.; Bertini, I.; Luchinat, C. *Nuclear and Electron Relaxation. The Magnetic Nucleus-Unpaired Electron Coupling in Solution*; VCH: Weinheim, Germany, 1991.
- Korb, J. P.; Ahadi, M.; Zientara, G. P.; Freed, J. H. Dynamic effects of pair correlation functions on spin relaxation by translational diffusion in two-dimensional fluids. *J. Chem. Phys.* **1987**, *86*, 1125–1130.
- Terreno, E.; Geninatti Crich, S.; Belfiore, S.; Biancone, L.; Cabella, C.; Esposito, G.; Manazza, A. D.; Aime, S. Effect of the intracellular localization of a Gd-based imaging probe on the relaxation enhancement of water protons. *Magn. Reson. Med.* **2006**, *55*(3), 491–7.
- Sieber, F.; Sieber-Blum, M. Dye-mediated photosensitization of murine neuroblastoma cells. *Cancer Res.* **1986**, *46*, 2072–2076.
- McGivan, J. D. Rat hepatoma cells express novel transport systems for glutamine and glutamate in addition to those present in normal rat hepatocytes. *Biochem. J.* **1998**, *330*, 255–260.
- Bode, B. P.; Fuchs, B. C.; Hurley, B. P.; Conroy, J. L.; Suetterlin, J. E.; Tanabe, K. K.; Rhoads, D. B.; Abcouwer, S. F.; Souba, W. W. Molecular and functional analysis of glutamine uptake in human hepatoma and liver-derived cells. *Am. J. Physiol.: Gastrointest. Liver Physiol.* **2002**, *283*, G1062–G1073.
- Cabella, C.; Geninatti Crich, S.; Corpillo, D.; Barge, A.; Ghirelli, C.; Bruno, E.; Lorusso, V.; Uggeri, F.; Aime, S. Cellular labeling with Gd(III) chelates: only high thermodynamic stabilities prevent the cells to act as “sponges” of Gd³⁺ ions. *Contrast Media Mol. Imaging* **2006**, *1*, 23–29.
- Collins, C. L.; Wasa, M.; Souba, W. W.; Abcouwer, S. F. Determinants of glutamine dependence and utilization by normal and tumor-derived breast cell lines. *J. Cell. Physiol.* **1998**, *176*, 166–178.
- Wasa, M.; Wang, H. S.; Okada, A. Characterization of L-glutamine transport by a human neuroblastoma cell line. *Am. J. Physiol.: Cell Physiol.* **2002**, *282*, C1246–C1253.

- (46) Dolinska, M.; Dybel, A.; Albrecht, J. Glutamine transport in C6 glioma cells. *Neurochem. Int.* **2000**, *37*, 139–146.
- (47) Van de Poll, M.; Soeters, P.; Deutz, N.; Fearon, K.; Dejong, C. Renal metabolism of amino acids: its role in interorgan amino acid exchange. *Am. J. Clin. Nutr.* **2004**, *79*, 185–197.
- (48) Boggio, K.; Di Carlo, E.; Rovero, S.; Cavallo, F.; Quaglino, E.; Lollini, P. L.; Nanni, P.; Nicoletti, G.; Wolf, S.; Musiani, P.; Forni, G. Ability of systemic interleukin-12 to hamper progressive stages of mammary carcinogenesis in HER2/neu transgenic mice. *Cancer Res.* **2000**, *60*, 359–364.
- (49) Nycomed Imaging A.S. Polyazacycloalkane Compounds. Patent WO96/28433, 1996.
- (50) Strom, C. S.; Michalopoulos, G. Collagen as a substrate for cell growth and differentiation. *Methods Enzymol.* **1982**, *82*, 544–555.
- (51) Probst, I.; Unthan-Fechner, K. Activation of glycolysis by insulin with a sequential increase of the 6-phosphofructo-2-kinase activity, fructose-2,6-bisphosphate level and pyruvate kinase activity in cultured rat hepatocytes. *Eur. J. Biochem.* **1985**, *153*, 347–353.
- (52) Geninatti Crich, S.; Biancone, L.; Cantaluppi, V.; Duo, D.; Esposito, G.; Russo, S.; Camussi, G.; Aime, S. Improved route for the visualization of stem cells labeled with a Gd-/Eu-chelate as dual (MRI and fluorescence) agent. *Magn. Reson. Med.* **2004**, *51*, 938–944.
- (53) Bradford, M. M. A rapid and sensitive method for the quantitation of microgram quantities of protein utilizing the principle of protein-dye binding. *Anal. Biochem.* **1976**, *72*, 248–254.

JM0601093